Received: 1 December 2017 | Accepted: 17 April 2018

DOI: 10.1002/hyp.13137

RESEARCH ARTICLE

WILEY

Groundwater recharge amidst focused stormwater infiltration

Aditi S. Bhaskar[1] | Dianna M. Hogan[2] | John R. Nimmo[3] | Kimberlie S. Perkins[3]

[1]Department of Civil and Environmental Engineering, Colorado State University, 1372 Campus Delivery, Fort Collins, CO 80521, USA

[2]Eastern Geographic Science Center, U.S. Geological Survey, 12201 Sunrise Valley Drive, MSN 521, Reston, VA 20192, USA

[3]Water Cycle Branch, U.S. Geological Survey, 345 Middlefield Road, Menlo Park, CA 94025, USA

Correspondence
Aditi Bhaskar, Department of Civil and Environmental Engineering, 1372 Campus Delivery, Colorado State University, Fort Collins, Colorado 80523, USA.
Email: aditi.bhaskar@colostate.edu

Funding information
Division of Earth Sciences, Grant/Award Number: 1349815

Abstract

Distributed, infiltration-based approaches to stormwater management are being implemented to mitigate effects of urban development on water resources. One of the goals of this type of storm water management, sometimes called low impact development or green infrastructure, is to maintain groundwater recharge and stream base flow at predevelopment levels. However, the connection between infiltration-based stormwater management and groundwater recharge is not straightforward. Water infiltrated through stormwater facilities may be stored in soil moisture, taken up by evapotranspiration or contribute to recharge and eventually base flow. This study focused on a 1.1 km^2 suburban, low impact development watershed in Clarksburg, Maryland, USA, that was urbanized and contained 73 infiltration-based stormwater facilities. Continuous water table measurements were used to quantify the movement of infiltrated stormwater. Time series analyses were performed on hydrographs of 7 wells, and the episodic master recession method was used. Persistence in water levels, as measured by autocorrelation function, was found to be positively related to depth to water. Storm properties (precipitation rate and duration) and well location (proximity to the nearest stream) were significant in driving episodic recharge to precipitation ratios. The well that had the highest recharge to precipitation ratios and water table rises of up to 1.5 m in response to storm events was located furthest from the stream and down gradient of stormwater infiltration locations. This work may be considered in evaluating the effects of planned watershed-scale infiltration-based stormwater management on groundwater flow systems.

KEYWORDS

green infrastructure, groundwater recharge, water table fluctuations

1 | INTRODUCTION

Groundwater recharge, the part of infiltrated water that reaches the water table, serves as a storage reservoir with delayed release between rain and stream flow. Urbanisation may lead to increase in groundwater recharge, but more often in humid settings, urbanization is expected to lead to reductions in recharge (Bhaskar et al., 2016). To mitigate the potential reduction in groundwater recharge due to urban development, recent approaches to stormwater management aim to increase recharge through distributed stormwater infiltration (Prince George's County, 1999; US EPA, 2000). This type of stormwater management is called low impact development (LID) when implemented on a watershed scale, and individual practices focused on infiltration are often termed *green infrastructure* (Fletcher et al., 2014). Since most implementations of green infrastructure are within existing urban development with conventional stormwater management, thus, far we have had few opportunities to evaluate changes to recharge resulting from watershed-scale implementations of stormwater infiltration (Jefferson et al., 2017).

Recharge can be highly spatially heterogeneous, even in nonurban areas, due to variations in topography (Delin, Healy, Landon, & Böhlke, 2000). Storm characteristics, such as magnitude, duration, rate, and intensity, also play a key role in determining what part of precipitation becomes recharge (Tashie, Mirus, & Pavelsky, 2016). Previous work

has used modelling to examine the potential effects of infiltration-based stormwater facilities on groundwater levels beneath individual facilities (e.g., Machusick, Welker, & Traver, 2011; Newcomer, Gurdak, Sklar, & Nanus, 2014) and resulting from multiple facilities (Barron, Barr, & Donn, 2013; Carleton, 2010; Endreny & Collins, 2009; Göbel et al., 2004; Holman-Dodds, Bradley, & Potter, 2003; Ku, Hagelin, & Buxton, 1992; Locatelli et al., 2017; Maimone, O'Rourke, Knighton, & Thomas, 2011; Shuster, Gehring, & Gerken, 2007; Stephens, Miller, Moore, Umstot, & Salvato, 2012; Trinh & Chui, 2013). One monitoring analysis of groundwater elevations indicated that the effect of stormwater infiltration facilities is small but significant in Back Bay, Boston (Thomas & Vogel, 2012), although in another case, the effect of stormwater infiltration on groundwater elevations was not detectible (Keßler, Meyer, Seeling, Tressel, & Krein, 2012).

Examining trends in stream base flow provides an aggregate measure of changes to groundwater recharge across an entire watershed and has demonstrated in our study area in Clarksburg, Maryland, USA, that base and total flow increased during urbanization using LID (Bhaskar, Hogan, & Archfield, 2016). As an integrator, however, stream base flow conceals information on the internal processing and distribution of water within the watershed. Water levels are one of the few hydrologic state variables—as opposed to fluxes such as streamflow, precipitation, and evapotranspiration—commonly measured that allow us to peer into processes within a watershed (Peterson & Western, 2014). The effect of stormwater infiltration on water table elevations is important to understand in the planning process for siting stormwater infiltration facilities in areas that do not lead to underground infrastructure flooding or other negative effects.

With the motivation of investigating the drivers of groundwater response to storm events within a watershed that was recently urbanized using LID, we seek to answer the following questions: (a) How does water level persistence and rate of recession vary across wells in this LID watershed? (b) What role do storm properties (precipitation magnitude, duration, and rate) and pre-event water level play, compared with spatial variability between wells, in driving recharge? To answer these questions, we examined correlations between water table fluctuations, storm properties, and well characteristics in a suburban watershed with numerous infiltration stormwater facilities, using time series analysis and the episodic master recession (EMR) method.

2 | METHODS

2.1 | Study area and well instrumentation

The climate in the study area, Clarksburg, Maryland, USA (Figure 1), is humid subtropical with an average 1,178 mm of rain per year. The study area is in the Piedmont physiographic province and is underlain by metamorphic rock (metasiltstone) with granular quartzite of the Marburg Formation (Southworth et al., 2007). The study area was previously agricultural and forested and between 2002 and 2010 was converted to residential suburban development with 30% impervious surface cover (Bhaskar, Hogan, & Archfield, 2016; Hogan, Jarnagin, Loperfido, & Van Ness, 2014). This suburban development employed infiltration-based stormwater facilities such as bio-retention facilities, dry swales, recharge chambers, storm drain recharge facilities, and drywell recharge facilities. Bio-retention facilities are vegetated depressions that allow for evapotranspiration, storage, and infiltration and have storage volumes between 34.5–100.2 m^3 (1,220–3,540 ft^3). Dry swales are linear channels that are covered with turf and soil filter systems, which temporarily store and then filter the desired treatment volume. They have a filter bed of prepared soil that overlays a perforated pipe underdrain system, which overlays a stone recharge trench. Recharge chambers are open-bottom chambers that allow infiltration into surrounding soil. In storm drain recharge facilities, also known as recharge trenches, the stormwater from the first 25 mm (1 in.) of the rain event enters a perforated pipe to allow the water to infiltrate, with an estimated storage volume ranging from 3.54–21.5 m^3 (125–760 ft^3). Dry well recharge facilities have gutters that drain roof run-off to an underground storage chamber for infiltration, with a minimum depth of 1.32 m (4 ft 4 in.) below land surface. There were 73 of these stormwater infiltration facilities in the area draining to the Tributary 104 stream gage (Figure 1), which treated approximately 25% of the impervious area in the watershed (drainage areas to these infiltration-based stormwater facilities are shown in Bhaskar, Hogan, and Archfield (2016)).

Seven wells in the study area were instrumented with Onset HOBO U20 L water level loggers (Figure 1; Table 1). Three of these wells were installed in 2002 (3, 4, and 6) by the Clarksburg Village Partnership. Three wells were installed in September 2014 (1, 2, and 5) using a hollow stem auger, with 5′ sections of 2″ slotted screens and developed by bailing before instrumenting. The Onset HOBO U20 L loggers recorded absolute pressure every 5 min for approximately 2 years. An additional Onset HOBO U20 L logger was deployed in air within the Well 2 casing to record barometric pressure. Monthly reference water level measurements (recorded in USGS NWIS) were used with the "Barometric Compensation Assistant" in Onset HOBO ware to convert the pressure measurements to depth to water level in all wells. We manually excluded occasional time periods from the analysis data set when the wells were used by others for water quality sampling.

2.2 | Time series analysis

Time series analyses of water levels have been previously used to understand the temporal properties of streamflow and water level records, often in karst settings (Crosbie, Binning, & Kalma, 2005; Duvert, Jourde, Raiber, & Cox, 2015; Herman, Toran, & White, 2009; Larocque, Mangin, Razack, & Banton, 1998; Lee & Lee, 2000; Lee, Yi, & Hwang, 2005; Massei et al., 2006). We used an autocorrelation analysis to investigate the degree of persistence (also called memory) in the water table elevation records. As calculations of autocorrelation require evenly spaced data, depth to water level data were linearly interpolated to standard 5-min increments between May 14, 2015 and February 28, 2017. Two periods of missing data at particular wells (July 5, 2015–July 15, 2015, at Well 3 and May 14, 2015–June 12, 2015 at Site 2) were filled with random normally distributed values with the mean and standard deviation taken from the rest of the water level records, as was done by Herman et al. (2009). The data were detrended to remove the sinusoidal, seasonal

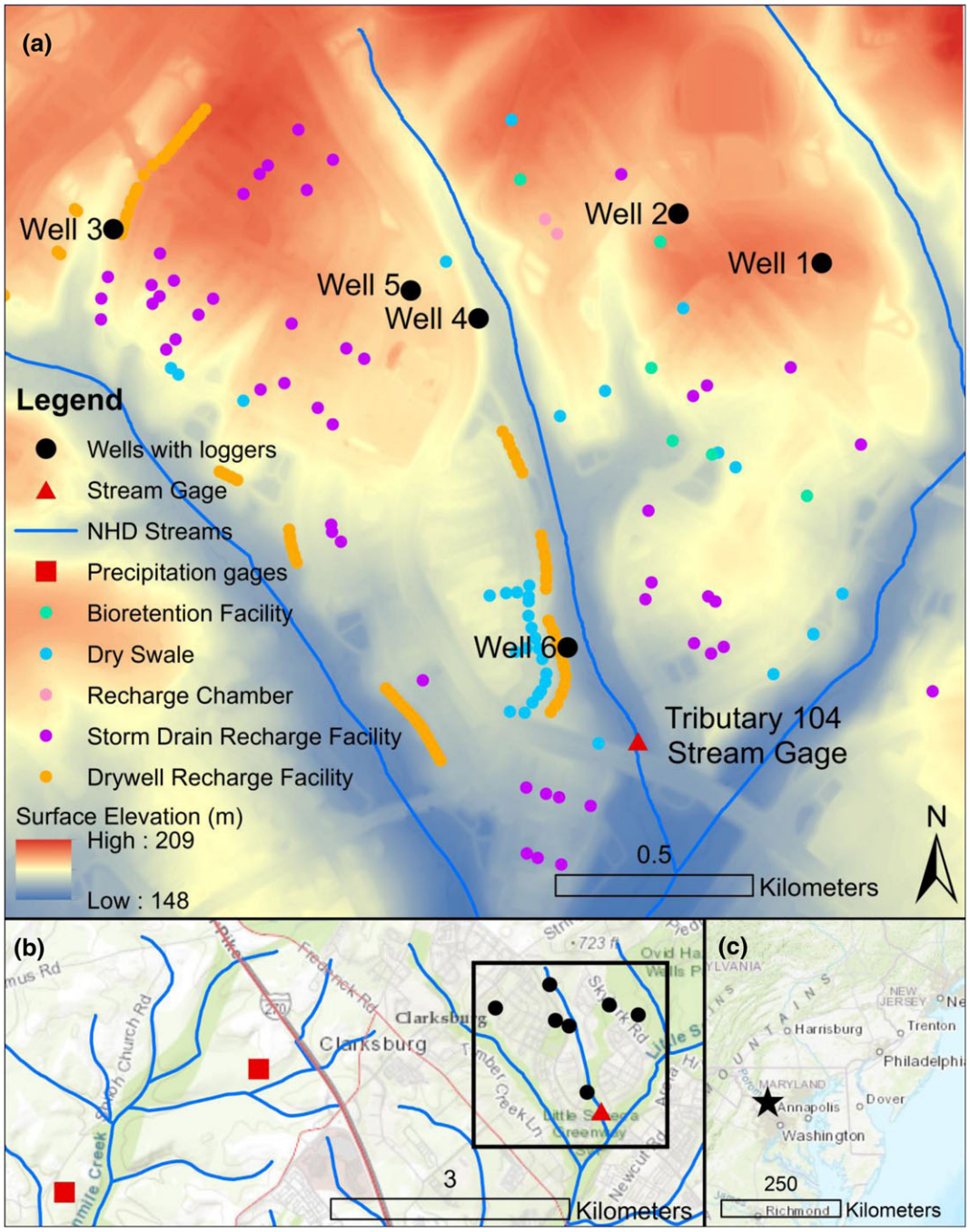

FIGURE 1 (a) Study area, locations of monitoring wells instrumented with water level loggers, infiltration-based storm water facilities, stream network from the National Hydrography Dataset, stream gage at tributary 104 (USGS 01644371), and elevation (m) from 2013 LiDAR. (b) Black rectangle shows the location of the study area inset shown in (a), as well as the precipitation gages used (USGS 391328077185901 and USGS 391407077174001). (c) Location of the study area in the mid-Atlantic United States

TABLE 1 Well names used in this manuscript, U.S. Geological Survey National Water Information System (USGS NWIS) site numbers, well depth, and mean water table elevation over the entire period of record at each well (Figure 2)

Well names	USGS NWIS site number	Land surface altitude (m)	Well depth (m)	Mean water table elevation (m)
1	391424077150601	191.4	18.0	176.2
2	391427077151701	187.1	14.2	176.2
5	391422077153901	181.1	10.4	175.0
3	391426077160401	182.6	10.6	174.8
4	391420077153401	175.8	7.8	168.8
6	391359077152601	162.9	10.9	158.1

pattern in the observed water levels, as well as any linear trend, in order to isolate the degree of persistence in water levels in response to storm events (Duvert et al., 2015; Herman et al., 2009). We carried out the detrending by subtracting the following fitted function from depth to water level records:

$$a + b\sin(2\pi T) + c\cos(2\pi T) + dT, \quad (1)$$

where a, b, c, and d are fitting parameters, and T is time. We used the lag, which corresponds to the autocorrelation coefficient of 0.2 to compare the degree of persistence between wells, as was done by previous researchers (Duvert et al., 2015; Imagawa, Takeuchi, Kawachi, Chono, & Ishida, 2013; Massei et al., 2006).

We analysed frequency components of the water table hydrographs using the function spectrum from the base package of the R programming language (R Core Team, 2016). Applying a fast Fourier transform to a gap-free portion of the water table hydrograph, this algorithm computes the spectral density of frequencies to indicate the relative preponderance of periodicities that contribute to the time-domain behaviour of the hydrograph. We applied a smoothing function to the results using a weighted average of nine consecutive points, four on each side of the point being evaluated. To facilitate interpretation of the time-scales of most importance, we computed reciprocals of frequency and plotted the spectral densities as a function of period.

2.3 | Water table fluctuation analysis

When recharge occurs in response to a particular event, for example a rainstorm, the water table elevation may rise temporarily before equilibrating as the recharge is redistributed. That rise, along with specific yield (also known as drainable porosity—the water drainage due to a unit drop in water table elevation), can define how much recharge led to the observed fluctuation in water table elevation (Equation (1); Healy, 2010):

$$R = S_y \times \Delta H, \quad (2)$$

where R is recharge (length dimensions), S_Y is specific yield (dimensionless), and H is water table elevation (length dimensionless). The water table fluctuation approach provides an estimate of episodic recharge, not total recharge, because recharge occurring in a steady way would not lead to observable fluctuations in water table elevation. The method also assumes predominantly one-dimensional flow to the saturated zone and has a spatial scale of 1–100 s of m^2 (Delin, Healy, Lorenz, & Nimmo, 2007).

A continuous approach for analysing water table fluctuations was presented by Crosbie et al. (2005), but we will use an event-based approach, called the EMR method (Nimmo, Horowitz, & Mitchell, 2015). The EMR method combines the water table fluctuation approach (Equation (2)) with a reproducible process to define and separately estimate recharge for individual storm events (https://wwwrcamnl.wr.usgs.gov/uzf/EMR_Method/EMR.method.html).

The EMR method uses a master recession curve (Heppner & Nimmo, 2005) to define the projected position of the water table if no storm events had occurred. When the observed water table elevation deviates from this projected recessing water table by a specified threshold (referred to as fluctuation tolerance), an episode of recharge is identified. The master recession curve was fitted to data from recession periods, which were selected by identifying times where neither weighing precipitation gage (Figure 1) was recording precipitation. For the EMR input data file, the two weighing precipitation gages (Figure 1; USGS 391328077185901 and USGS 391407077174001) were averaged and then linearly interpolated to match the times when water level data were recorded at each well. We assumed rainfall within the watershed was spatially uniform. We did not use the criterion that the water table should be recessing (dH/dT < 0), because some noise around 0 is expected, and removing only positive values of dH/dT would lead to a negative bias (a similar issue is discussed by Kirchner (2009) for streamflow recession analysis). The relationship between H and dH/dT for recession periods was then fit to a line:

$$\frac{dH}{dT_{recession}} = m^* H_{recession} + b, \quad (3)$$

where H is water table elevation (m), T is time (days), and m and b are the fitted slope and intercept parameters, respectively.

To calculate the amounts of both precipitation and recharge from individual storms, the EMR method requires specification of specific yield, lag time (delay time between the incidence of water at the land surface and its effect on the water table), fluctuation tolerance, and an optional moving average smoothing parameter, in addition to the slope and intercept parameters of the linear dH/dT versus H fit used as the master recession curve. In determining the master recession parameters, H(T) data within a poststorm interval called the storm recovery time were excluded as presumably affected by continuing recharge in addition to recessional processes. Specific yield (S_y) was assumed to be 0.01, based on an estimate at a nearby basin in the Potomac River watershed (Trainer & Watkins, 1975). Since estimated recharge scales directly with S_y (Equation (2)), this parameter was held constant across wells to compare relative storm response, and we did not want to assume variability between wells when we did not have knowledge of that variability. Fluctuation tolerance was the one parameter that was varied between wells, because the water level records had different levels of "smoothness" versus "jaggedness". The fluctuation tolerance values were manually adjusted so as to make the number, length, dates of storm episodes identified as recharge events as consistent as possible between wells. The resulting fluctuation tolerance values were 0.25 m/day for Well 3, 0.09 m/day for Well 4, 0.13 m/day for Well 6, and 0.19 m/day for Well 5. The manual optimization of lag time and fluctuation tolerance was easily achieved because of their near-independence and known cause-and-effect interpretation. The optimized values represent a direct quantification of the hydrologic judgments entailed in hydrograph-evaluation techniques. The optimized storm recovery time was 1.75 days, the lag time 1.1 days, and the moving average smoothing parameter 120 due to the fine temporal resolution of water table elevation data. The time period analysed for EMR was May 14, 2015, to February 28, 2017, because of the near-continuous data at four wells, which had clear storm-event responses in water table elevations (Wells 3–6).

The drivers of the recharge to precipitation ratio (RPR) for each storm event at each well, derived from the EMR method, were analysed using multiple linear regression (Equation (4)).

$$\begin{aligned}\log(RPR) = {} & \beta_0 + \beta_1 \log(\textit{average precipitation rate}) \\ & + \beta_2(\textit{episode duration}) \\ & + \beta_3(\textit{pre-event head difference from mean}) \\ & + \beta_4\ (\textit{well 3}) + \beta_5\ (\textit{well 4}) + \beta_6\ (\textit{well 6}) + \varepsilon, \end{aligned} \quad (4)$$

where β_0 is the model intercept, $\beta_{1\text{-}6}$ are model coefficients, Wells 3, 4, and 6 are binary variables (one if the episode takes place at the given well, and zero otherwise), and ε is unexplained variation. Well 5 was not included as a binary predictor variable because if the variables Well 3, Well 4, and Well 6 are all zero, indicating the episode did not take place at those wells, then this would indicate the episode occurred at Well 5. The prediction variable was transformed to *log(RPR)* because model residuals versus predicted untransformed RPR values were observed to be heteroscedastic and nonlinear, whereas a logarithmic transformation achieved more linear and constant variance residuals. The explanatory variable average precipitation rate was also transformed because of nonlinearity between this variable and RPR.

3 | RESULTS

The depth to water time series (Figure 2) showed markedly different seasonal and event response patterns across the watershed. The well with the deepest water table below land surface (1, not to be confused with the lowest water table elevation at Well 6, also see Table 1) showed a water table that was primarily driven by longer term patterns of wetting and drying and a strong seasonal signal. For example, the rise in water table in the fall of 2015 occurred months later at Well 1 than at wells with shallower depths to water. There were few distinct responses to individual storm events at Well 1. Well 2 had a shallower water table but showed overall similarity to Well 1, with more identifiable responses to storm events. The four wells with intermediate depth to water (Wells 3–6) were analysed with the EMR method because they showed clear and discrete responses to storm events, which overlay broader, seasonal fluctuations. Storm-driven water table rises did not scale directly with depth to water. For example, during most storms, Well 3 had the largest magnitude increase in water table response to individual storm events but was at an intermediate to deep range in terms of depth to water table compared with the other six wells (Figure 2). These patterns are explored further with time series analysis and the EMR method.

3.1 | Time series analysis

Lags that corresponded to an autocorrelation coefficient of 0.2 (referred to as $k_{0.2}$) are plotted in Figure 3. Figure 3 shows that $k_{0.2}$ was better explained by mean depth to water (Figure 3a, adjusted R^2 0.17), where the wells with deeper water tables showed a greater temporal water table persistence, as compared with distance to stream (Figure 3b, adjusted R^2–0.23), although neither of the relationships shown was significant.

Spectral analysis of the longest gap-free record across wells (June 12, 2015–July 5, 2016) is shown in Figure 4. All wells showed an approximately linear relationship in spectral density with period on this log–log scale, which corresponds to the commonly reported power relationship between spectral density of water table records and period on a linear scale (Duvert et al., 2015; Herman et al., 2009; Imagawa et al., 2013).

There were peaks in spectral density at a period of about 0.5 days for all wells, which was most pronounced for Well 4 and least for Wells 3 and 6. There also were peaks at a period of 1 day for Wells 1, 2, 4, and 6. The heightened cyclicality at these periods may relate to demand or barometric pressure changes. Similar peaks at nearly the same periods were observed by Herman et al. (2009). Well 3 had a relatively high spectral density for periods greater than about 0.3 day, as expected given its strongly pronounced fluctuations. This characteristic suggests an especially high sensitivity to water inputs at this location. Wells 1 and 2 had comparatively high spectral

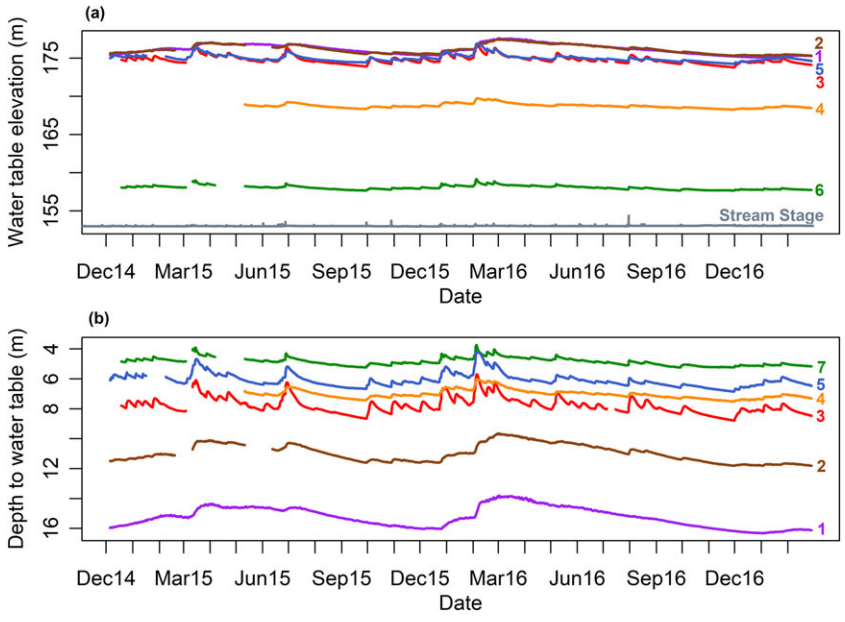

FIGURE 2 (a) Water table elevation (m) and (b) depth to water below land surface (m) between December 2014 and February 2017 at six instrumented wells (Figure 1). On (a), stream stage elevation (m) at tributary 104 is also plotted (https://waterdata.usgs.gov/usa/nwis/uv?01644371)

densities at periods greater than about 40 days and comparatively low densities at shorter periods, whereas the opposite pattern was observed at Wells 4 and 6. These patterns correspond to the lesser sensitivity to high-frequency fluctuations visible in the Wells 1 and 2 hydrographs (Figure 2). A possible cause is that the greater thickness of the unsaturated zone at Wells 1 and 2 increases its effectiveness for damping out short-term fluctuations occurring at the land surface.

3.2 | Water table fluctuations

After examining the water table fluctuations from a continuous perspective with the autocorrelation function and spectral analysis (Figures 3 and 4), we then examined individual storm events using the EMR method for water table fluctuations. This approach required the creation of a master recession curve for each well, predicting the expected rate of decrease in water table elevation (dH/dT) across water table elevations (H; Figure 5). Using a test for differences in slopes (Larsen & Marx, 2012: 572), we found the recession slope for Well 3 was significantly smaller than that of Wells 4, 5, and 6 (all p values were <1e-5), and the recession slope for Well 4 was greater than that of Wells 5 and 6 (p values were <1e-4), whereas the slopes for Wells 5 and 6 were not significantly different. Well 3 had the fastest recession (most negative value for dH/dT), which can also be seen by examination of recession periods in Figure 2, and the recession rate at Well 4 was the most gradual.

These master recession curves were used to identify recharge episodes using the EMR code. The water table rise for each episode was multiplied by specific yield to result in recharge for each episode, which is plotted against precipitation magnitude for each episode in Figure 6a. Changes in the assumed value of specific yield would shift the points in Figure 6a uniformly up or down. If the specific yield increased, some episodes would have a RPR > 1, which is possible for areas where recharge is occurring not only as a result of precipitation in the vicinity of the well but also due to nearby collection and recharge of stormwater, which fell as precipitation over a larger drainage area. Changes to specific yield that kept a constant value across the watershed would preserve the relative position between wells.

From inspection of Figure 6a, it appears that in addition to scatter, recharge at Well 3 was generally higher than at other wells for the same precipitation magnitude. This was examined further by dividing the episode recharge (mm) by episode precipitation (mm) to calculate the RPR (Figure 6b). We observed that Well 3 had the highest median RPR, followed by Wells 5, 6, and 4, which corresponded to the size of water table rises seen in Figure 2. We tested whether the differences between wells in Figure 6b were statistically significant. Applying the nonparametric Kruskal–Wallis rank test lead us to reject the null hypothesis that the distribution of RPR was identical across wells (p value of 8e-6). A pairwise Wilcoxon rank-sum test was used to test the hypothesis that pairwise comparisons between wells were from the same distribution. We found significant differences between RPR of Well 3 and the other three wells (p values <.05), whereas the other comparisons were found not to have significant differences. Since RPR is directly proportional to Sy, the significant differences in RPR among wells could also be explained by Sy values that are 3 times higher in Wells 4–6 compared with Well 3.

We examined potential drivers of the RPR (Figure 7), which could explain the scatter in the relationship between precipitation and recharge (Figure 6b). RPR was found to be negatively related to episode precipitation magnitude and episode precipitation rate (Figures 7a and 7b). RPR was positively related to episode duration and pre-event water table elevations (Figures 7c and 7d). These relations were modelled using multiple linear regression (Equation (4)). Both episode

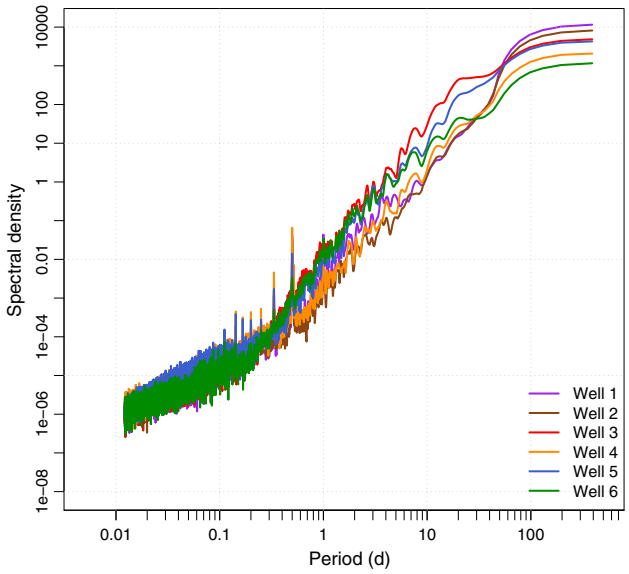

FIGURE 4 Spectral density versus period (days), calculated using the gap-free period June 12, 2015–July 5, 2016

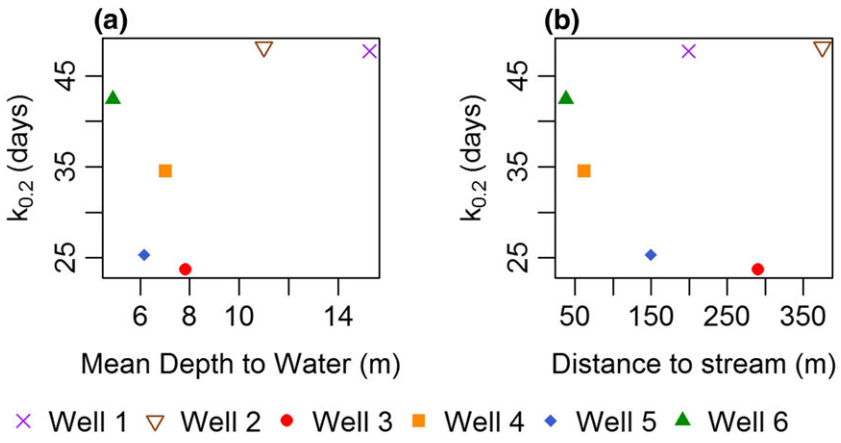

FIGURE 3 (a) Lag (days) corresponding to an autocorrelation of 0.2 ($k_{0.2}$) versus mean depth to water (m). (b) Lag (days) corresponding to an autocorrelation of 0.2 ($k_{0.2}$) versus distance from well to nearest stream (m)

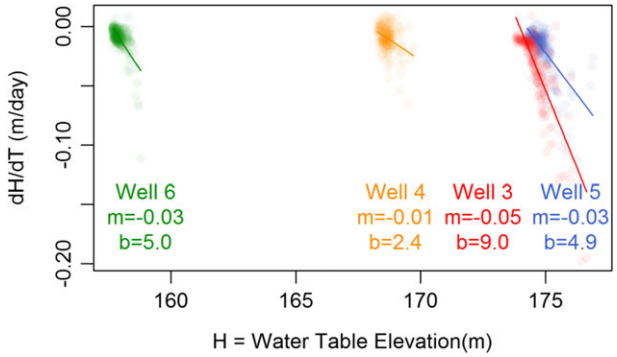

FIGURE 5 Change in water table elevation over time (dH/dT, where H is water table elevation and T is time, in m/day) versus water table elevation (H) at each well. The coloured dots represent the observations considered for the recession fit, and the coloured lines represent the fits to the observations (i.e., the master recession curves). The slope (m) and intercept (b) values for each fitted master recession curve (Equation (3)) is also given

precipitation and average precipitation rate could not be included in the model because of the high degree of collinearity between these variables (Variance Inflation Factor >80). Including average precipitation rate resulted in a higher adjusted R^2 and lower Predicted Residual Error Sum of Squares compared with including episode precipitation, which is why average precipitation rate was included, and episode precipitation was not. The adjusted R^2 for the model was 0.87 with a p value <2.2e-16. All model coefficients were found to be significant (Table 2).

The model coefficients (Table 2) indicated that higher precipitation rate and recharge occurring at Well 4 or 6 reduced RPR, whereas longer duration, higher pre-event water table elevation, and an episode occurring at Well 3 increased RPR. The explanatory variables that produced the largest change in RPR (measured by standardized coefficients, not shown) were average precipitation rate, occurring at Well 4 and occurring at Well 6. The pre-event water table elevation difference from mean had the smallest standardized coefficient,

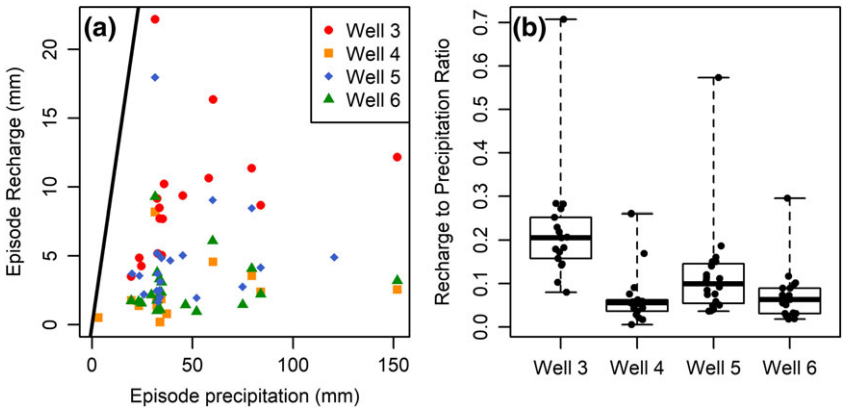

FIGURE 6 (a) Each recharge episode identified is plotted as a single point, with recharge over the episode (mm) versus precipitation over the entire episode (mm). The 1:1 line is plotted as a thick black line. (b) Recharge to precipitation ratio for events. Each episode is plotted as a dot, which overlays the summary statistics represented as a boxplot for the recharge to precipitation ratios at each well

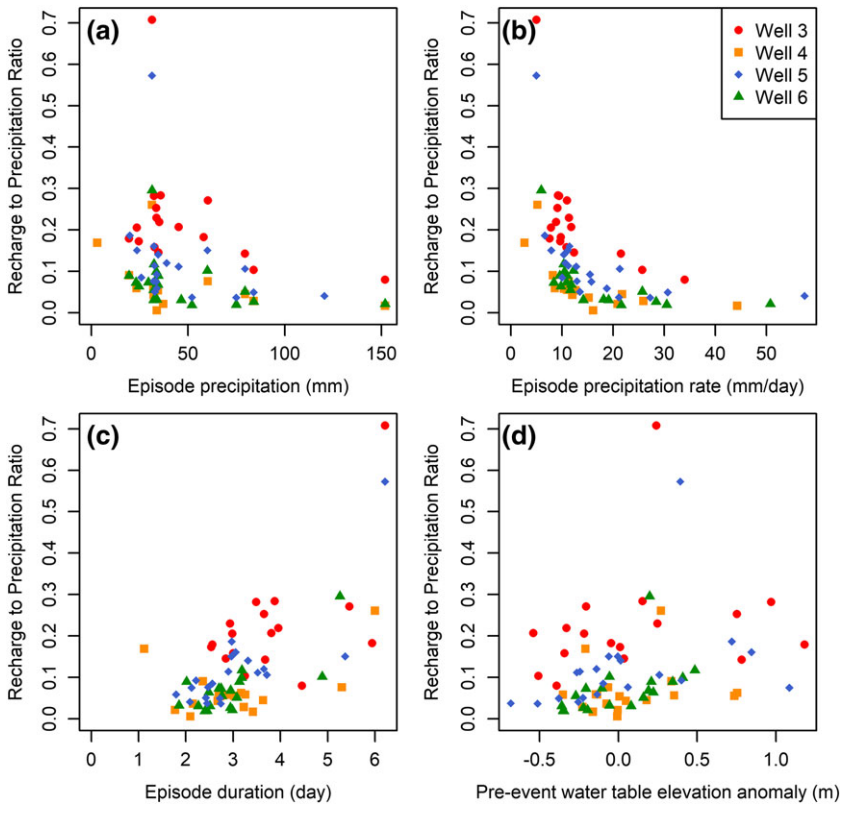

FIGURE 7 (a) Recharge to precipitation ratio (RPR) for each episode versus episode total precipitation magnitude (mm). (b) RPR versus episode average precipitation rate (mm/day). (c) RPR versus episode duration (days). (d) RPR versus pre-event water table elevation anomaly represents the water table elevation before the storm event minus mean water table elevation for each well (m)

indicating the relatively low importance of this variable in explaining RPR. Median RPR was also related to the proximity of the well to a stream (Figure 8a) and not as closely related to the proximity of the well to a stormwater infiltration facility (Figure 8b) and the mean depth to water (Figure 8c).

4 | DISCUSSION

a) How does water level persistence and rate of recession vary across wells in this low impact development watershed?

Previous studies found that downstream wells along the axis of the stream (Duvert et al., 2015) or wells at the toe of the alluvial fan (Imagawa et al., 2013) have greater persistence in water table records. Persistence was related to mean depth to water (Figure 3a), which fits with a conceptual model of thicker unsaturated zones damping discrete signals from the land surface, although depth to water did not describe all the variability observed (Figure 8c). For example, Well 3 had the lowest persistence but had a relatively deep depth to water (Figure 3a). Well 3 also had a faster recession rate than the other wells (Figure 5).

b) What role do storm properties (precipitation magnitude, duration, and rate) and pre-event water level play, compared with spatial variability between wells, in driving recharge?

TABLE 2 Coefficient estimates, associated explanatory variable, and *p* values associated with the coefficients in the multiple linear regression model of Equation (4)

Coefficient	Associated explanatory variable	Coefficient estimate	*p* value
β_0	Intercept	−0.84	2e-3
β_1	Log (average precipitation rate)	−0.86	<2e-16
β_2	Episode duration	0.24	8e-9
β_3	Pre-event water table elevation difference from mean	0.26	.01
β_4	Well 3	0.36	1e-3
β_5	Well 4	−0.78	1e-10
β_6	Well 6	−0.47	1e-15

Well 3 also stood out as having a significantly higher RPR (Figure 6b). For all wells, RPR were negatively related to average precipitation rate and positively related to episode duration and water table elevation before the storm (Table 2). RPR were also positively related to occurring at Well 3. Multiple factors could have contributed to the higher RPR observed at Well 3. Both Wells 3 and 6 were within forested valleys, down gradient of single family houses with drywells—systems where a roof gutter downspout collected run-off from the back half of a roof and channelled that water to an underground gravel pit. The stormwater collected by a drywell was from a small area (half an individual roof), but the drywells were numerous and close to Wells 3 and 6 (drywell recharge facilities were within 20 m of both wells; Figure 8b). The infiltration from these drywells could be hypothesized to lead to larger water table fluctuations, but the effect at these two wells was found to be dissimilar (Figure 6b). Proximity to a stream may be a contributor to the dissimilar water table responses observed at these two wells. As shown in a hypothetical MODFLOW model (Risser, Gburek, & Folmar, 2005), wells close to streams had a damped water table fluctuation, even with the same recharge, because of the faster groundwater drainage near the stream—similar to the effect of a constant head boundary condition nearby. Well 6 was 38 m away from a perennial stream (Figure 1; Figure 8), which would be expected to constrain water table fluctuations, whereas Well 3 was in a valley of a different stream that was usually dry and was 290 m away from a perennial stream.

4.1 | Implications

Many of the same factors driving RPR in North Carolina (Tashie et al., 2016) were found to be important here. Tashie et al. (2016) also found a negative correlation between RPR and precipitation magnitude and rate and a positive correlation between RPR and duration, an effect that was more pronounced in developed versus undeveloped areas. The decrease in RPR with larger magnitude events (Figure 7a) was expected due to greater dominance of overland flow in large magnitude storms (Tashie et al., 2016). We would expect that in an urban area with infiltration of stormwater, there would be greater RPR at low magnitude events compared with conventionally developed urban watersheds without focused infiltration of stormwater. This greater RPR compared with conventional urban watersheds might not hold for large magnitude storm events because infiltration-based

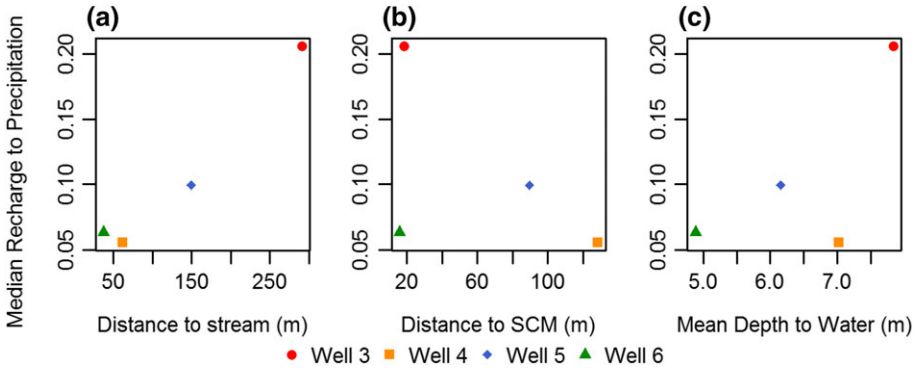

FIGURE 8 Median recharge to precipitation ratio at each well across all storm episodes versus (a) distance from each well to the nearest stream (m), (b) distance from each well to the nearest infiltration storm water control measure (SCM; m), and (c) mean depth to water (m)

stormwater facilities are generally constructed with a certain storage capacity, past that additional stormwater becomes overland flow or enters stormwater pipes through overflow or bypass structures. This limited capacity of infrastructure for infiltration might imply that for large magnitude events the RPR of LID and conventional urban watersheds would become similar, because the stormwater facilities are no longer serving as enhanced infiltration pathways. Although we observed a decrease in RPR with precipitation magnitude, we were not able to test how this relationship would have been different compared with an urban watershed without the managed infiltration of stormwater, due to the lack of data in a comparison watershed at the same time. Our study was an observational one, where we investigated relations between properties of water level records, storm properties, and landscape parameters, but because we could not change spatial properties of our study watershed, we could not identify precise causes in between-well variations in water table behaviour. We found significant variability in recharge response between wells above and beyond the effects of storm characteristics (Table 2), which could have been caused by hydrogeologic properties, contributions from stormwater infiltration, and topographic position.

5 | SUMMARY AND CONCLUSIONS

a) Persistence in water levels and their spectral density of frequencies were related to mean depth to water (Figure 3a; Figure 4). Storm event pulses of recharge were expected to be more diffuse in time and depth for wells with thicker unsaturated zones. Storm-generated water table responses of these wells were generally more subdued and more autocorrelated over longer lengths of time, with lesser representation of high-frequency components.

b) Four wells in our study area (Wells 3–6) were analysed with the EMR method for water table fluctuations (Nimmo et al., 2015). We found that these wells had significantly different RPR (Figure 6b). Well 3, located in a valley down gradient from infiltration facilities and also the greatest distance from a stream out of the four, had the largest RPR (Figure 6b). In addition to having the largest water table increases in response to storm events, Well 3 had the fastest water table recession (Figure 5).

c) RPR were significantly lower for storms that were shorter, at a higher precipitation rate, and had lower water table elevations before the storm (Figure 7; Table 2). Wells that were further from streams had a larger recharge response (Figure 8a).

This work has implications for the planning phase of stormwater management, when the locations of stormwater infiltration facilities are being sited. In areas where the water table is shallow enough to cause potential concerns for infrastructure with groundwater mounding, the placement of stormwater infiltration facilities to avoid these issues becomes important. In an ameliorating factor, because of the damping effect of the stream on water table fluctuations, the wells closest to the stream, with generally shallower water tables, are expected to rise less in response to recharge events compared with wells further from the stream. Much deeper water tables may not respond to individual storm events because of the thickness of the unsaturated zone. Areas of the watershed at intermediate depth-to-water levels, the exact ranges of which will likely vary with climate and hydrogeologic conditions, may have the largest water table response to episodic recharge events.

ACKNOWLEDGMENTS

We gratefully acknowledge Environmental Systems Analysis and Montgomery County Department of Environmental Protection for permission to instrument wells maintained by them; H. Tarekegn, K. Hopkins, C. Wright, B. Hammond, and M. Metes for assistance with field work; J. Grey for well installation; S. Sparkman for GIS assistance; B. Mirus and anonymous reviewers for helpful comments. This work was carried out with support from NSF-EAR Postdoctoral Fellowship (1349815) to A. S. Bhaskar. This work builds on the Clarksburg Integrated Study Partnership between US Environmental Protection Agency, Montgomery County Department of Environmental Protection, the US Geological Survey, and the University of Maryland. The stream gage data referenced within have been funded in part by the USEPA under agreements DW14921533, DW14922385 to the USGS. The data presented in this article are publicly available through the CUAHSI Water Data Center at http://hiscentral.cuahsi.org/pub_network.aspx?n=5616.

ORCID

Aditi S. Bhaskar http://orcid.org/0000-0001-9803-4003

REFERENCES

Barron, O. V., Barr, A. D., & Donn, M. J. (2013). Effect of urbanisation on the water balance of a catchment with shallow groundwater. *Journal of Hydrology*, *485*, 162–176. https://doi.org/10.1016/j.jhydrol.2012.04.027

Bhaskar, A. S., Beesley, L., Burns, M. J., Fletcher, T. D., Hamel, P., Oldham, C. E., & Roy, A. H. (2016). Will it rise or will it fall? Managing the complex effects of urbanization on base flow. *Freshwater Science*, *35*(1), 293–310. https://doi.org/10.1086/685084

Bhaskar, A. S., Hogan, D. M., & Archfield, S. A. (2016). Urban base flow with low impact development. *Hydrological Processes*, *30*(18), 3156–3171. https://doi.org/10.1002/hyp.10808

Carleton GB. 2010. Simulation of groundwater mounding beneath hypothetical storm water infiltration basins. U.S Geological Survey Scientific Investigations Report 2010–5102.

Crosbie, R. S., Binning, P., & Kalma, J. D. (2005). A time series approach to inferring groundwater recharge using the water table fluctuation method. *Water Resources Research*, *41*(1). https://doi.org/10.1029/2004WR003077

Delin, G. N., Healy, R. W., Landon, M. K., & Böhlke, J. K. (2000). Effects of topography and soil properties on recharge at two sites in an agricultural Field 1. *JAWRA Journal of the American Water Resources Association*, *36*(6), 1401–1416. https://doi.org/10.1111/j.1752-1688.2000.tb05735.x

Delin, G. N., Healy, R. W., Lorenz, D. L., & Nimmo, J. R. (2007). Comparison of local-to regional-scale estimates of groundwater recharge in Minnesota, USA. *Journal of Hydrology*, *334*(1–2), 231–249. https://doi.org/10.1016/j.jhydrol.2006.10.010

Duvert, C., Jourde, H., Raiber, M., & Cox, M. E. (2015). Correlation and spectral analyses to assess the response of a shallow aquifer to low

and high frequency rainfall fluctuations. *Journal of Hydrology*, *527*, 894–907. https://doi.org/10.1016/j.jhydrol.2015.05.054

Endreny, T., & Collins, V. (2009). Implications of bioretention basin spatial arrangements on storm water recharge and groundwater mounding. *Ecological Engineering*, *35*(5), 670–677. https://doi.org/10.1016/j.ecoleng.2008.10.017

Fletcher, T. D., Shuster, W., Hunt, W. F., Ashley, R., Butler, D., Arthur, S., … Viklander, M. (2014). SUDS, LID, BMPs, WSUD and more —The evolution and application of terminology surrounding urban drainage. *Urban Water Journal*, *12*, 1–18. https://doi.org/10.1080/1573062X.2014.916314

Göbel, P., Stubbe, H., Weinert, M., Zimmermann, J., Fach, S., Dierkes, C., … Coldewey, W. G. (2004). Near-natural storm water management and its effects on the water budget and groundwater surface in urban areas taking account of the hydrogeological conditions. *Journal of Hydrology*, *299*(3–4), 267–283.

Healy, R. W. (2010). *Estimating groundwater recharge*. Cambridge University Press.

Heppner CS, Nimmo JR. 2005. A computer program for predicting recharge with a master recession curve. USGS Numbered Series 2005–5172. Available at: http://pubs.er.usgs.gov/publication/sir20055172 [Accessed 6 May 2016]

Herman, E. K., Toran, L., & White, W. B. (2009). Quantifying the place of karst aquifers in the groundwater to surface water continuum: A time series analysis study of storm behavior in Pennsylvania water resources. *Journal of Hydrology*, *376*(1–2), 307–317. https://doi.org/10.1016/j.jhydrol.2009.07.043

Hogan, D., Jarnagin, S. T., Loperfido, J. V., & Van Ness, K. (2014). Mitigating the effects of landscape development on streams in urbanizing watersheds. *Journal of the American Water Resources Association*, *50*(1), 163–178. https://doi.org/10.1111/jawr.12123

Holman-Dodds, J. K., Bradley, A. A., & Potter, K. W. (2003). Evaluation of hydrologic benefits of infiltration based urban storm water management. *Journal of the American Water Resources Association*, *39*(1), 205–215. https://doi.org/10.1111/j.1752-1688.2003.tb01572.x

Imagawa, C., Takeuchi, J., Kawachi, T., Chono, S., & Ishida, K. (2013). Statistical analyses and modeling approaches to hydrodynamic characteristics in alluvial aquifer. *Hydrological Processes*, *27*(26), 4017–4027. https://doi.org/10.1002/hyp.9538

Jefferson, A. J., Bhaskar, A. S., Hopkins, K. G., Fanelli, R., Avellaneda, P. M., & McMillan, S. K. (2017). Storm water management network effectiveness and implications for urban watershed function: A critical review. *Hydrological Processes*, *31*(23), 4056–4080. https://doi.org/10.1002/hyp.11347

Keßler, S., Meyer, B., Seeling, S., Tressel, E., & Krein, A. (2012). Influence of near-to-nature storm water management on the local water balance using the example of an urban development area. *Water Environment Research*, *84*(5), 441–451. https://doi.org/10.2175/106143012X13347678384729

Kirchner, J. W. (2009). Catchments as simple dynamical systems: Catchment characterization, rainfall-runoff modeling, and doing hydrology backward. *Water Resources Research*, *45*(2). W02429

Ku, H. F. H., Hagelin, N. W., & Buxton, H. T. (1992). Effects of urban storm-runoff control on ground-water recharge in Nassau County, New York. *Ground Water*, *30*(4), 507–514. https://doi.org/10.1111/j.1745-6584.1992.tb01526.x

Larocque, M., Mangin, A., Razack, M., & Banton, O. (1998). Contribution of correlation and spectral analyses to the regional study of a large karst aquifer (Charente, France). *Journal of Hydrology*, *205*(3), 217–231.

Larsen, R. J., & Marx, M. L. (2012). *An introduction to mathematical statistics and its applications*. Boston: Prentice Hall.

Lee, J.-Y., & Lee, K.-K. (2000). Use of hydrologic time series data for identification of recharge mechanism in a fractured bedrock aquifer system. *Journal of Hydrology*, *229*(3–4), 190–201. https://doi.org/10.1016/S0022-1694(00)00158-X

Lee, J.-Y., Yi, M.-J., & Hwang, D. (2005). Dependency of hydrologic responses and recharge estimates on water-level monitoring locations within a small catchment. *Geosciences Journal*, *9*(3), 277–286. https://doi.org/10.1007/BF02910588

Locatelli, L., Mark, O., Mikkelsen, P. S., Arnbjerg-Nielsen, K., Deletic, A., Roldin, M., & Binning, P. J. (2017). Hydrologic impact of urbanization with extensive storm water infiltration. *Journal of Hydrology*, *544*, 524–537. https://doi.org/10.1016/j.jhydrol.2016.11.030

Machusick, M., Welker, A., & Traver, R. (2011). Groundwater mounding at a storm-water infiltration BMP. *Journal of Irrigation and Drainage Engineering*, *137*(3), 154–160. https://doi.org/10.1061/(ASCE)IR.1943-4774.0000184

Maimone, M., O'Rourke, D., Knighton, J., & Thomas, C. (2011). Potential impacts of extensive storm water infiltration in Philadelphia. *Environmental Engineer and Scientist: Applied Research and Practice*, *14*, 29–39.

Massei, N., Dupont, J. P., Mahler, B. J., Laignel, B., Fournier, M., Valdes, D., & Ogier, S. (2006). Investigating transport properties and turbidity dynamics of a karst aquifer using correlation, spectral, and wavelet analyses. *Journal of Hydrology*, *329*(1–2), 244–257. https://doi.org/10.1016/j.jhydrol.2006.02.021

Newcomer, M. E., Gurdak, J. J., Sklar, L. S., & Nanus, L. (2014). Urban recharge beneath low impact development and effects of climate variability and change. *Water Resources Research*, *50*(2), 1716–1734. https://doi.org/10.1002/2013WR014282

Nimmo, J. R., Horowitz, C., & Mitchell, L. (2015). Discrete-storm water-table fluctuation method to estimate episodic recharge. *Groundwater*, *53*(2), 282–292. https://doi.org/10.1111/gwat.12177

Peterson, T. J., & Western, A. W. (2014). Nonlinear time-series modeling of unconfined groundwater head. *Water Resources Research*, *50*(10), 8330–8355. https://doi.org/10.1002/2013WR014800

Prince George's County. 1999. Low-Impact Development Hydrologic Analysis Available at: http://water.epa.gov/polwaste/green/upload/lidnatl.pdf

R Core Team. 2016. R: A Language and Environment for Statistical Computing. R Foundation for Statistical Computing: Vienna, Austria. Available at: https://www.r-project.org/

Risser DW, Gburek WJ, Folmar GJ. 2005. Comparison of methods for estimating ground-water recharge and base flow at a small watershed underlain by fractured bedrock in the eastern United States. US Department of the Interior, US Geological Survey. Available at: http://pubs.usgs.gov/sir/2005/5038/ [Accessed 26 June 2015]

Shuster, W. D., Gehring, R., & Gerken, J. (2007). Prospects for enhanced groundwater recharge via infiltration of urban storm water runoff: A case study. *Journal of Soil and Water Conservation*, *62*(3), 129–137.

Southworth S, Brezinski DK, Burton WC, Froelich AJ, Reddy JE, Denenny D, Daniels DL. 2007. Geologic Map of the Frederick 30′ X 60′ Quadrangle, Maryland, Virginia, and West Virginia Available at: http://pubs.usgs.gov/sim/2889/ [Accessed 26 May 2015]

Stephens, D. B., Miller, M., Moore, S. J., Umstot, T., & Salvato, D. J. (2012). Decentralized groundwater recharge systems using roof water and storm water runoff. *Journal of the American Water Resources Association*, *48*(1), 134–144. https://doi.org/10.1111/j.1752-1688.2011.00600.x

Tashie, A. M., Mirus, B. B., & Pavelsky, T. M. (2016). Identifying long-term empirical relationships between storm characteristics and episodic groundwater recharge. *Water Resources Research*, *52*(1), 21–35. https://doi.org/10.1002/2015WR017876

Thomas, B. F., & Vogel, R. M. (2012). Impact of storm water recharge practices on Boston groundwater elevations. *Journal of Hydrologic Engineering*, *17*(8), 923–932. https://doi.org/10.1061/(ASCE)HE.1943-5584.0000534

Trainer FW, Watkins FA. 1975. Geohydrologic reconnaissance of the upper Potomac River basin. US Geological Survey Water-Supply Paper 2035. Available at: https://pubs.er.usgs.gov/publication/wsp2035 [Accessed 30 January 2017]

Trinh, D. H., & Chui, T. F. M. (2013). Assessing the hydrologic restoration of an urbanized area via an integrated distributed hydrological model. *Hydrology and Earth System Sciences*, *17*(12), 4789–4801. https://doi.org/10.5194/hess-17-4789-2013

US EPA. 2000. Low impact development (LID) literature review and fact sheets. US EPA Document # EPA-841-B-00-005. Available at: http://water.epa.gov/polwaste/green/lidlit.cfm [Accessed 7 July 2015]

How to cite this article: Bhaskar AS, Hogan DM, Nimmo JR, Perkins KS. Groundwater recharge amidst focused stormwater infiltration. *Hydrological Processes*. 2018;1–11. https://doi.org/10.1002/hyp.13137